

Spontaneous dimerization in the spin-1 bilinear-biquadratic Heisenberg model on a honeycomb lattice

Yu-Wen Lee* and Min-Fong Yang

Department of Physics, Tunghai University, Taichung 40704, Taiwan

(Dated: December 10, 2018)

Within the linear flavor-wave theory, we show that, due to the quantum order-by-disorder mechanism, the spin-1 bilinear-biquadratic Heisenberg model on a honeycomb lattice can spontaneously develop a columnar dimer order with a non-bipartite structure. The low-lying excitations above this novel ground state form several flat bands separated by nonzero energy gaps. Our results suggest that the quantum phase transition separating this dimerized phase with the nearby Néel-order phase may be of first order.

PACS numbers: 75.10.Jm, 75.30.Kz 75.10.Kt,

Quantum spin systems on various kinds of lattices have provided a wide playground for the search of novel quantum states and quantum phase transitions. It has been proposed that, in some spin-1/2 systems on a square lattice, quantum paramagnetic phases with valence-bond-solid order can emerge and their transitions to the anti-ferromagnetic Néel states may belong to the deconfined quantum criticality.^{1,2} On a honeycomb lattice, even the more fascinating quantum spin-liquid state has recently been proposed and even observed in the half-filled Hubbard model and related frustrated spin-1/2 Heisenberg models.³⁻⁵

Rich physics is also expected in quantum spin systems with larger spin moments. Prominent examples include the spin-1 bilinear-biquadratic (BLBQ) model described by the Hamiltonian

$$H = \sum_{\langle i,j \rangle} \left[J (\mathbf{S}_i \cdot \mathbf{S}_j) + K (\mathbf{S}_i \cdot \mathbf{S}_j)^2 \right] \quad (1)$$

with a bilinear exchange coupling $J \equiv \cos \theta$ and a biquadratic exchange coupling $K \equiv \sin \theta$, where the parameter θ controls the ratio of these two couplings. It has been shown that quantum phases with either collinear or noncollinear nematic order can appear in this spin system.^{6,7} In these nematic phases, dipolar spin order parameters vanish, $\langle \mathbf{S} \rangle = 0$, but spin rotation symmetry is spontaneously broken due to nonzero quadrupolar spin expectation values, $\langle S^\alpha S^\beta + S^\beta S^\alpha \rangle \neq 0$ ($\alpha, \beta = x, y, z$). Here we focus on the parameter region with $\pi/4 \leq \theta < \pi/2$ (i.e., $K \geq J > 0$), where the noncollinear nematic states described by mutually orthogonal nematic directors are expected at the mean-field level.^{6,7} When the BLBQ model is defined on a triangular lattice, in which each site has 6 neighbors, the ground state is found to possess a three-sublattice nematic order.^{8,9} The nematic directors on the three sublattices A, B, and C of the triangular lattice are orthogonal to each other (say, along the x , y , and z directions, respectively). On the other hand, if this model is placed on a square lattice, because of the smaller coordination number for this lattice structure, there are not enough constraints to uniquely determine a set of mutually orthogonal nematic directors.

Therefore, the expected noncollinear nematic state will form a highly degenerate ground-state manifold. Usually, such macroscopic degeneracy at the variational level can be lifted by quantum effects, and a unique ground state will be selected by the order-by-disorder mechanism. Following this reasoning, the ground state for the BLBQ model with $J = K$ on a square lattice has been analyzed recently by means of a semiclassical flavor-wave theory and exact diagonalizations.¹⁰ It is found that instead of the naive two-sublattice state, the ground state develops an unexpected three-sublattice long-range order, even though this system is defined on a bipartite lattice and with only nearest-neighbor interactions.

Since the honeycomb lattice has an even smaller coordination number, one may wonder whether it can support ground states quite different from those on a square lattice. A possible candidate of the quantum phase for the BLBQ model on a honeycomb lattice with $\pi/4 \leq \theta < \pi/2$ (i.e., $K \geq J > 0$) has been proposed.¹¹ By employing the tensor renormalization group method^{12,13} under the assumption that the ground-state wave function can be described by a periodic tensor network with elementary hexagon as the unit cell, the ground state is found to have plaquette valence-bond-solid (PVBS) order. This PVBS state breaks the lattice translational symmetry but preserves the spin SU(2) symmetry. However, due to the assumed periodicity for their variational states, the possibilities for the ground states to display more complicated structures are missed in their exploration. Hence their results may not be conclusive.

In the present work, we determine the nature of the ground state of the BLBQ model in Eq. (1) with $K \geq J > 0$ on a honeycomb lattice using the linear flavor-wave (LFW) theory.^{6,7,14,15} Previous studies on the cases of the square lattice have proved the validity and success of this approach.^{10,16} In Ref. 10, the conclusion of the LFW analysis for the square-lattice case was shown to be supported by the exact diagonalization calculations for systems of finite sizes.¹⁰ Besides, the results within the LFW theory for the SU(4) Heisenberg model provide useful guides for numerical methods to uncover the intricate dimerized structure and color ordering of the ground state.¹⁶ For the present case of the spin-1 BLBQ

model on a honeycomb lattice, following the reasoning of these works, we find that the ground states exhibit exotic columnar dimer order [see Fig. 1(c)] and break spontaneously both the spin $SU(2)$ symmetry and the lattice translation symmetry. Our results arise from the order-by-disorder mechanism, where the ground states are selected among the degenerate manifold of the noncollinear nematic states by minimizing the zero-point energies of quantum fluctuations. We note that the unit cell of the resulting ground-state pattern is quite large (consisting of 18 lattice sites), while the underlying lattice is bipartite. Within our LFW analysis, the flavor-wave excitations in the present systems are found to be localized, and the low-lying modes form several flat bands separated by nonzero energy gaps. This observation is rather different from the usual cases with spontaneous $SU(2)$ symmetry breaking. Moreover, it is found that the gapful ground state with columnar dimer order remains even in the limit of $J = K$ (or $\theta = \pi/4$), at which a direct transition to the nearby antiferromagnetic phase for $J > K$ is anticipated.^{6,7} This suggests that the quantum phase transition at $J = K$, which separates these two phases with distinct types of long-range order, may be of first order. The implication of our results on generalized models is discussed at the end of this Rapid Communication.

The LFW theory starts from representing the model in Eq. (1) in terms of three-flavor Schwinger bosons $a_{i,\alpha}$ under the local constraint $\sum_{\alpha} a_{i,\alpha}^{\dagger} a_{i,\alpha} = 1$,

$$H = \sum_{\langle i,j \rangle} \left[J \chi_{ij}^{\dagger} \chi_{ij} + (K - J) \Delta_{ij}^{\dagger} \Delta_{ij} + (K - J) \right]. \quad (2)$$

Here we define two bond operators, $\chi_{ij} = \sum_{\alpha} a_{i,\alpha}^{\dagger} a_{i,\alpha} a_{j,\alpha}$ and $\Delta_{ij} = \sum_{\alpha} a_{i,\alpha} a_{j,\alpha}$. The Schwinger bosons $a_{i,\alpha}^{\dagger}$ (with $\alpha = x, y, z$) create three time-reversal-invariant local basis states, $|x\rangle = \frac{1}{\sqrt{2}}(|s_z = 1\rangle - |s_z = -1\rangle)$, $|y\rangle = \frac{i}{\sqrt{2}}(|s_z = 1\rangle + |s_z = -1\rangle)$, and $|z\rangle = |s_z = 0\rangle$. In terms of these bosons, the spin operators become $S_{i,\alpha} = -i \sum_{\beta,\gamma} \epsilon_{\alpha\beta\gamma} a_{i,\beta}^{\dagger} a_{i,\gamma}$. The first step is the mean-field analysis based on a site-factorized variational wave function. At this mean-field level, the Schwinger-boson operators $\mathbf{a}_i \equiv (a_{i,x}, a_{i,y}, a_{i,z})$ are replaced by a (complex) three-component vector \mathbf{d}_i , and the energy of the nearest-neighbor bond $\langle i, j \rangle$ is minimal when the two vectors \mathbf{d}_i and \mathbf{d}_j are mutually orthogonal.^{6,7} The mean-field ground state configuration is highly degenerate on a honeycomb lattice, and as can be seen from Eq. (2), the associated mean-field energy per bond is $(K - J)$. This macroscopic degeneracy can be lifted when quantum fluctuations above each mean-field state are included. Within the LFW analysis, the leading quantum corrections to the mean-field energy of the considered variational state come from the zero-point energy of the LFW Hamiltonian. Therefore, the configuration with the lowest zero-point energy will be picked out as the true ground state. This is in essence a quantum order-by-disorder selection mechanism.

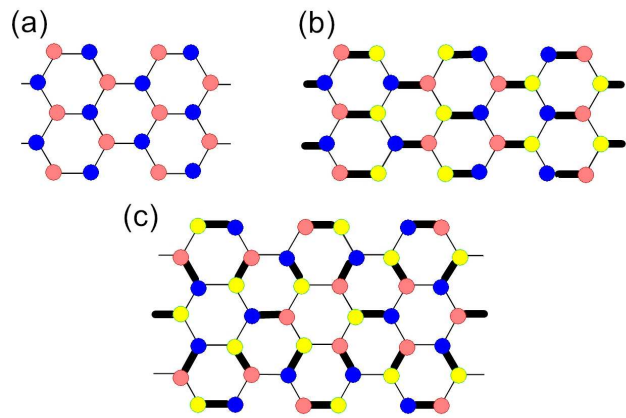


FIG. 1: (Color online) Schematic representation of three possible candidates for the ground state: (a) two-sublattice state and (b) staggered dimer state, both of which have higher LFW energies; (c) columnar dimer state selected by quantum fluctuations within the LFW theory. Here the three mutually orthogonal vectors \mathbf{d}_i in the mean-field analysis are denoted by the unit vectors along the x , y , and z directions, and are associated with different colors. Strong bonds with the lowest zero-point energy are denoted by thick lines. The remaining weak bonds are depicted by thin lines.

The derivation of the LFW Hamiltonian proceeds as follows. For a given configuration of the variational state, when the two classical vectors on a nearest-neighbor bond $\langle i, j \rangle$ are, say, $\mathbf{d}_i = \hat{x}$ and $\mathbf{d}_j = \hat{y}$ (named as the XY bond in the following), we approximate semiclassically their Schwinger-boson operators by $\mathbf{a}_i \simeq (1, a_{i,y}, a_{i,z})$ and $\mathbf{a}_j \simeq (a_{j,x}, 1, a_{j,z})$. The operators $a_{i,y}$ and $a_{i,z}$ on site i ($a_{j,x}$ and $a_{j,z}$ on site j) describe the quantum fluctuations around the classical vectors, and they play the role of the Holstein-Primakoff bosons in the usual spin-wave theory. Therefore, up to the linear order in these operators, the bond operators become

$$\chi_{ij} \simeq a_{i,y}^{\dagger} + a_{j,x}, \quad \Delta_{ij} \simeq a_{i,y} + a_{j,x}. \quad (3)$$

Substituting them into the Hamiltonian in Eq. (2), we obtain the desired quadratic LFW Hamiltonian.

We note that the LFW Hamiltonian in general consists of a sum of independent parts that describe the motion of bosons on certain connected clusters. For example, for a given nearest-neighbor bond (say, the XY bond), when all of the \mathbf{d} vectors of its surrounding sites are orthogonal (say, $\mathbf{d}_i = \hat{z}$) to *both* \mathbf{d} vectors on that bond, the 2 bosons (say, the x and y components of the Schwinger bosons) within that bond cannot move to neighboring sites. That is, the motion of these bosons becomes decoupled from the surrounding of that bond, and it can be described by a 2-site Hamiltonian. In the following, such 2-site clusters are dubbed as strong bonds and denoted by thick lines in Figs. 1(b) and 1(c). On the other hand, the remaining bonds depicted by thin lines can be linked to from larger cluster and they are termed as weak bonds. As discussed below, we find that the zero-point energy

(and therefore the ground-state energy) is minimized for those strong bonds. Therefore, we expect that the states with the lowest zero-point energy should be the ones that contain as many strong bonds as possible. Such a “maximum strong bond rule,” which has been noted in other context,¹⁶ forms our main guiding principle in searching for possible candidates of the ground state. Based on this observation, in addition to the two-sublattice state [Fig. 1(a)], which is the naive ground-state configuration on the present bipartite lattice, we consider two more configurations. They are the staggered dimer state and the columnar dimer state [Figs. 1(b) and Figs. 1(c), respectively], both of which contain the maximum number of strong bonds per elementary hexagon. Nevertheless, as discussed in the paragraph below Eq. (6), the zero-point energy for weak bonds in the columnar dimer state is lower than that in the staggered dimer state. Thus the columnar dimer state in Fig. 1(c) with a more complicated structure is selected by the zero-point quantum fluctuations within the LFW theory.

Now we begin to derive the explicit expressions of the zero-point energies for the three configurations shown in Fig. 1. For the case of the two-sublattice state formed by XY bonds only, the z components of the Schwinger bosons play no role and the LFW Hamiltonian reduces to an effective model for the two-component boson mixture on a single connected cluster of the whole honeycomb lattice. By means of the Bogoliubov transformation, the excitation spectrum of the resulting quadratic bosonic Hamiltonian can be easily obtained. This results in the following ground-state energy per site (i.e., the sum of the mean-field energy density and the zero-point contribution), $E_G = \frac{1}{N} \sum_{\mathbf{k}} (\lambda_{1\mathbf{k}} + \lambda_{2\mathbf{k}})$. Here N is the number of lattice sites, \mathbf{k} runs over the first Brillouin zone of the honeycomb lattice, and $\lambda_{1,2}(\mathbf{k}) = \sqrt{(\varepsilon_0 \pm |\Delta_{2\mathbf{k}}|)^2 - |\Delta_{1\mathbf{k}}|^2}$ with $\varepsilon_0 = \frac{z}{2}K$, $\Delta_{1\mathbf{k}} = \frac{z}{2}J\gamma_{\mathbf{k}}$, and $\Delta_{2\mathbf{k}} = \frac{z}{2}(K - J)\gamma_{\mathbf{k}}$. The coordination number $z = 3$ for the honeycomb lattice, and $\gamma_{\mathbf{k}} = \frac{1}{z} \sum_{\delta} e^{i\mathbf{k}\cdot\delta}$, where δ runs over the three nearest-neighbor vectors, $\delta_1 = (1, 0)$, $\delta_2 = (-\frac{1}{2}, \frac{\sqrt{3}}{2})$, and $\delta_3 = (-\frac{1}{2}, -\frac{\sqrt{3}}{2})$.

Unlike the two-sublattice state, both the staggered dimer state and the columnar dimer state have strong bonds. Besides, their weak bonds form many one-dimensional zig-zag chains or 6-site clusters (hexagonal loops) as shown in Fig. 1(b) and Fig. 1(c), respectively. Since the bosons on these weak bonds are decoupled from those on the strong bonds, these bosons can be described by an effective Hamiltonian on a one-dimensional chain of $2N_c$ bonds, where $N_c \rightarrow \infty$ and $N_c = 3$ for the staggered dimer state and the columnar dimer state, respectively. That is, the flavor-wave excitations are well localized within those chains or clusters. Because the LFW Hamiltonians on clusters of different sizes give distinct contributions to the zero-point energy, they need to be considered separately. For a given strong bond, by diagonalizing the corresponding 2-site LFW Hamiltonian, its

ground-state energy can be found as

$$E_{s\text{-bond}} = \sqrt{K(K - J)}. \quad (4)$$

Similarly, for excitations localized within a closed chain of $2N_c$ bonds, diagonalization of the corresponding one-dimensional Hamiltonian results in the following expression for the ground-state energy per weak bond,

$$E_{w\text{-bond}}(N_c) = \frac{1}{2N_c} \sum_k \left[\tilde{\lambda}_1(k) + \tilde{\lambda}_2(k) \right]. \quad (5)$$

Here the one-dimensional momentum $k = \frac{2\pi n}{N_c}$ with $n = 1, \dots, N_c$, $\tilde{\lambda}_{1,2}(k) = \sqrt{(\tilde{\varepsilon}_0 \pm |\tilde{\Delta}_{2k}|)^2 - |\tilde{\Delta}_{1k}|^2}$ with $\tilde{\varepsilon}_0 = K$, $|\tilde{\Delta}_{1k}| = J|\cos(\frac{k}{2})|$, and $|\tilde{\Delta}_{2k}| = (K - J)|\cos(\frac{k}{2})|$. As seen from Figs. 1(b) and 1(c), in both the staggered dimer state and the columnar dimer state, the three nearest-neighbor bonds for each lattice site contain one strong and two weak bonds. Therefore, from Eqs. (4) and (5), the expression of the ground-state energy per site for both cases becomes

$$E_G = \frac{1}{2} E_{s\text{-bond}} + E_{w\text{-bond}}(N_c). \quad (6)$$

Thus the difference in energies between the staggered dimer state and the columnar dimer state comes from the contribution of the weak bonds. From Eq. (5), one can show that the energy per weak bond is an increasing function of N_c . In other words, the localized flavor-wave excitations residing on shorter chains will give a smaller contribution in Eq. (6). As mentioned above, $N_c = 3$ for the columnar dimer state and $N_c \rightarrow \infty$ for the staggered dimer state. Hence, we conclude that the former has a lower energy. Note that on a honeycomb lattice, the shortest closed loop of weak bonds is nothing but the hexagonal one with $N_c = 3$. Thus we conclude that the columnar dimer state should be the true ground state among the degenerate manifold.

The ground-state energy densities for the three types of states are presented in Fig. 2. We find that their energies become degenerate and approach to $3/2$ in the $\theta \rightarrow \pi/2$ limit. This comes from the fact that the mean-field state becomes an exact eigenstate at $\theta = \pi/2$ (or $J = 0$ and $K = 1$) and quantum fluctuations play no role here. Thus the mean-field energy per site $E_G = \frac{z}{2}(K - J) = 3/2$ is nothing but the exact energy eigenvalue. Moreover, our Fig. 2 shows that the columnar dimer state does have the lowest energy in the whole parameter regime $\pi/4 \leq \theta = \tan^{-1}(K/J) < \pi/2$. We note that the PVBS states proposed in Ref. 11 lie outside the degenerate manifold of the noncollinear nematic states and thus are not considered within the employed approach. However, we can compare their variational energies with those discussed in the present work. It is found that the ground-state energies of our columnar dimer states are also lower than those of the PVBS states. For instance, at the $SU(3)$ point with $\theta = \pi/4$ (or $J = K = 1/\sqrt{2}$), our

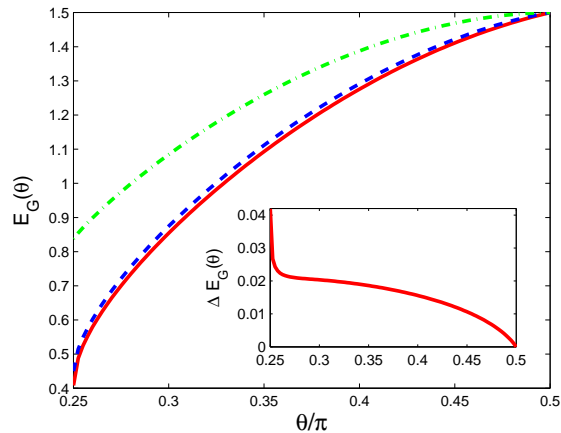


FIG. 2: (Color online) Ground state energy densities (per site) for the three states shown in Fig. 1 as a function of $\theta = \tan^{-1}(K/J)$. The dash-dotted, dashed, and solid lines are for the two-sublattice, the staggered dimer, and the columnar dimer states, respectively. Inset: Energy difference (per site) $\Delta E_G \equiv E_{G,\text{staggered dimer}} - E_{G,\text{column dimer}}$ between the staggered dimer and the columnar dimer states as a function of θ .

values of E_G for the two-sublattice state, the staggered dimer state, and the columnar dimer state are 0.8381 , $\sqrt{2}/\pi$ ($\simeq 0.4502$), and $1/\sqrt{6}$ ($\simeq 0.4082$), respectively. However, the energy density at $\theta = \pi/4$ for the PVBS state is about 0.536 , which is higher than the values for both of the dimerized states. Thus our calculations show that the peculiar dimerized ground states that spontaneously break both spatial and spin $SU(2)$ symmetries can in fact be energetically more favorable. We should stress that since the energies obtained within the LFW theory are not variational, the above comparison in energy may not be used to exclude the PVBS states as the true ground state. Nevertheless, the present investigation indicates that our dimerized states should at least be possible candidates.

To provide guides for future numerical investigations, some comments are discussed below. People usually perform exact diagonalization calculations for systems of finite sizes to obtain unbiased results and then provide numerical verification for analytical proposals. Since the unit cell of our columnar dimer state contains 18 lattice sites, large systems with sizes of several unit cells should be considered in order to deliver meaningful results complementary to our present work. But the required computational resources may make such calculations unlikely. In this regard, numerical variational approaches, such as the variational Monte Carlo method and the tensor network method, may be more promising, because their size limitation is less severe. Even in this case, our results show that one has to use the variational states compatible with the spatial structure of our columnar dimer state to determine convincingly the true ground state.

In addition to determining the nature of the ground

state within parameter regime $\pi/4 < \theta < \pi/2$, our results also help to characterize the types of phase transitions out of this phase. It is known that at the mean-field level, a phase transition to the nearby ferromagnetic phase occurs at $\theta = \pi/2$.^{6,7} At this value of θ , we find that the energy of the columnar dimer state ($E_G = 3/2$) is identical to that of the ferromagnetic state [see Eq. (1) with $\mathbf{S}_i = 1$]. Because these two states belong to different subspaces of the total spin, this agreement in energy indicates a level crossing and thus a first-order transition at $\theta = \pi/2$. On the other hand, the mean-field theory predicts a direct transition at $\theta = \pi/4$ from the noncollinear nematic to the antiferromagnetic phases.^{6,7} In our work, the effects of quantum fluctuations are taken into account under the LFW analysis. We find that there exist only the localized flavor-wave excitations above the columnar dimer state and these excitations form flat bands separated by nonzero energy gaps. Moreover, the gapful ground state with nonvanishing columnar dimer order persists even in the limit of $\theta = \pi/4$ (or $J = K$). This suggests that the quantum phase transition at $J = K$, which separates these two phases with distinct types of long-range order, should be of first order.

Finally, the implication of our results on generalized models is discussed. Unlike its counterparts on other lattices with larger coordination numbers z [i.e., the three-sublattice antiferromagnetic state on a triangular lattice^{8,9} ($z = 6$) and the three-sublattice stripelike state on a square lattice¹⁰ ($z = 4$)], the columnar dimer state on a honeycomb lattice ($z = 3$) has a solidlike pattern and supports only localized flavor-wave excitations within the LFW analysis. In addition, a conclusion similar to ours is reached for an $SU(4)$ -symmetric spin model with 4 states in the local Hilbert space.¹⁶ From all these findings, one may conclude that for generalized models with more local states [say, the $SO(n)$ bilinear-biquadratic model¹⁸⁻²⁰] and/or on two-dimensional lattices with smaller z , ground states with solid-like structures will be stabilized due to the same order-by-disorder mechanism. While this observation is based on the LFW analysis, we believe that the qualitative picture will not be modified even if higher quantum corrections are included.

To summarize, by employing the LFW theory, we show that the columnar dimer state is the ground state of the spin-1 BLBQ model on a honeycomb lattice with $\pi/4 < \theta < \pi/2$. We stress that our investigations are not of purely academic interest. In fact, at $\theta = \pi/4$ (i.e., $K = J > 0$), the present model possesses an enlarged $SU(3)$ symmetry and can be considered as an effective model for the Mott-insulating state of three-flavor cold fermions with one particle per lattice site.¹⁰ Therefore, our conclusions at this $SU(3)$ point may be examined experimentally for such cold fermions on a honeycomb optical lattice.¹⁷

Y.-W.L. and M.-F.Y. acknowledge the support from the National Science Council of Taiwan under Grants No. NSC 99-2112-M-029-004-MY3 and No. NSC 99-2112-M-

029-003-MY3, respectively.

-
- * Electronic address: ywlee@thu.edu.tw
- ¹ T. Senthil, A. Vishwanath, L. Balents, S. Sachdev, and M. P. A. Fisher, *Science* **303**, 1490 (2004).
 - ² T. Senthil, L. Balents, S. Sachdev, A. Vishwanath, and M. P. A. Fisher, *Phys. Rev. B* **70**, 144407 (2004).
 - ³ Z. Y. Meng, T. C. Lang, S. Wessel, F. F. Assaad, and A. Muramatsu, *Nature (London)* **464**, 847 (2010).
 - ⁴ F. Wang, *Phys. Rev. B* **82**, 024419 (2010)
 - ⁵ B. K. Clark, D. A. Abanin, and S. L. Sondhi, *Phys. Rev. Lett.* **107**, 087204 (2011).
 - ⁶ N. Papanicolaou, *Nucl. Phys. B* **305**, 367 (1988).
 - ⁷ For a recent review, see K. Penc and A. M. Läuchli, in *Introduction to Highly Frustrated Magnetism*, Vol. 164 of Springer Series in Solid-State Sciences, edited by C. Lacroix, P. Mendels and F. Mila (Springer, New York, 2011), pp. 331–360.
 - ⁸ H. Tsunetsugu and M. Arikawa, *J. Phys. Soc. Jap.* **75**, 083701 (2006).
 - ⁹ A. Läuchli, F. Mila, and K. Penc, *Phys. Rev. Lett.* **97**, 087205 (2006).
 - ¹⁰ T. A. Tóth, A. M. Läuchli, F. Mila, and K. Penc, *Phys. Rev. Lett.* **105**, 265301 (2010).
 - ¹¹ H. H. Zhao, Cenke Xu, Q. N. Chen, Z. C. Wei, M. P. Qin, G. M. Zhang, T. Xiang, arXiv:1105.2716v2.
 - ¹² H. C. Jiang, Z. Y. Weng, and T. Xiang, *Phys. Rev. Lett.* **101**, 090603 (2008); Z. Y. Xie, H. C. Jiang, Q. N. Chen, Z. Y. Weng, and T. Xiang, *ibid.* **103**, 160601 (2009).
 - ¹³ G. Vidal, *Phys. Rev. Lett.* **98**, 070201 (2007); J. Jordan, R. Orús, G. Vidal, F. Verstraete, and J. I. Cirac, *ibid.* **101**, 250602 (2008).
 - ¹⁴ A. Chubukov, *J. Phys. Condens. Matter* **2**, 1593 (1990).
 - ¹⁵ A. Joshi, M. Ma, F. Mila, D.N. Shi, and F.C. Zhang, *Phys. Rev. B* **60**, 6584 (1999).
 - ¹⁶ P. Corboz, A. M. Läuchli, K. Penc, M. Troyer, and F. Mila, *Phys. Rev. Lett.* **107**, 215301 (2011).
 - ¹⁷ G. Grynberg, B. Lounis, P. Verkerk, J. Y. Courtois, and C. Salomon, *Phys. Rev. Lett.* **70**, 2249 (1993). S.-L. Zhu, B. Wang, and L. M. Duan, *ibid.* **98**, 260402 (2007).
 - ¹⁸ H.-H. Tu, G.-M. Zhang, and T. Xiang, *Phys. Rev. B* **78**, 094404 (2008); *J. Phys. A: Math. Theor.* **41**, 415201 (2008).
 - ¹⁹ F. Alet, S. Capponi, H. Nonne, P. Lecheminant, and I. P. McCulloch, *Phys. Rev. B* **83**, 060407(R) (2011).
 - ²⁰ H.-H. Tu and R. Orús, *Phys. Rev. Lett.* **107**, 077204 (2011).